ORIGINAL ARTICLE

Journal of Cachexia, Sarcopenia and Muscle 2024; **15**: 255–269
Published online 7 December 2023 in Wiley Online Library (wileyonlinelibrary.com) **DOI:** 10.1002/jcsm.13398

DBC1 maintains skeletal muscle integrity by enhancing myogenesis and preventing myofibre wasting

Na Liang[1], Jia He[1], Jiaqi Yan[1], Xueying Han[1], Xiaoqian Zhang[1], Yamei Niu[2,3,4,5], Wuga Sha[1] & Jun Li[1]*

[1]*State Key Laboratory of Common Mechanism Research for Major Diseases, Institute of Basic Medical Sciences, Chinese Academy of Medical Sciences and Peking Union Medical College, Beijing, China;* [2]*Department of Pathology, Institute of Basic Medical Sciences, Chinese Academy of Medical Sciences, Beijing, China;* [3]*School of Basic Medicine, Peking Union Medical College, Beijing, China;* [4]*Neuroscience Center, Chinese Academy of Medical Sciences, Beijing, China;* [5]*Molecular Pathology Research Center, Chinese Academy of Medical Sciences and Peking Union Medical College, Beijing, China*

Abstract

Background Skeletal muscle atrophy, particularly ageing-related muscular atrophy such as sarcopenia, is a significant health concern. Despite its prevalence, the underlying mechanisms remain poorly understood, and specific approved medications are currently unavailable. Deleted in breast cancer 1 (DBC1) is a well-known regulator of senescence, metabolism or apoptosis. Recent reports suggest that DBC1 may also potentially regulate muscle function, as mice lacking DBC1 exhibit weakness and limpness. However, the function of DBC1 in skeletal muscle and its associated molecular mechanisms remain unknown, thus prompting the focus of this study.

Methods Tibialis anterior (TA) muscle-specific DBC1 knockdown C57BL/6J male mice were generated through a single injection of 2.00 E + 11 vg of adeno-associated virus 9 delivering single-guide RNA for DBC1. Grip strength and endurance were assessed 2 months later, followed by skeletal muscle harvest. Muscle atrophy model was generated by cast immobilization of the mouse hindlimb for 2 weeks. Molecular markers of atrophy were probed in muscles upon termination. Cardiotoxin (CTX) was injected in TA muscles of DBC1 knockdown mice, and muscle regeneration was assessed by immunohistochemistry, quantitative PCR and western blotting. DBC1 knockdown C2C12 cells and myotubes were investigated using immunofluorescence staining, Seahorse, immunohistology, fluorescence-activated cell sorting and RNA-sequencing analyses.

Results DBC1 knockdown in skeletal muscle of young mice led to signatures of muscle atrophy, including a 28% reduction in muscle grip force ($P = 0.023$), a 54.4% reduction in running distance ($P = 0.002$), a 14.3% reduction in muscle mass ($P = 0.007$) and significantly smaller myofibre cross-sectional areas ($P < 0.0001$). DBC1 levels decrease in age-related or limb immobilization-induced atrophic mouse muscles and overexpress DBC1-attenuated atrophic phenotypes in these mice. Muscle regeneration was hampered in mice with CTX-induced muscle injury by DBC1 knockdown, as evidenced by reductions in myofibre cross-sectional areas of regenerating myofibres with centralized nuclei ($P < 0.0001$), percentages of $MyoG^+$ nuclei ($P < 0.0001$) and fusion index ($P < 0.0001$). DBC1 transcriptionally regulated mouse double minute 2 (MDM2), which mediated ubiquitination and degradation of forkhead box O3 (FOXO3). Increased FOXO3 proteins hampered myogenesis in DBC1 knockdown satellite cells by compromising around 50% of mitochondrial functions ($P < 0.001$) and exacerbated atrophy in DBC1 knockdown myofibres by activating the ubiquitin–proteasome and autophagy–lysosome pathways.

Conclusions DBC1 is essential in maintaining skeletal muscle integrity by protecting against myofibres wasting and enhancing muscle regeneration via FOXO3. This research highlights the significance of DBC1 for healthy skeletal muscle function and its connection to muscular atrophy.

Keywords DBC1; FOXO3; myogenesis; skeletal muscle atrophy

Received: 14 April 2023; Revised: 27 September 2023; Accepted: 2 November 2023
**Correspondence to: Jun Li, State Key Laboratory of Common Mechanism Research for Major Diseases, Institute of Basic Medical Sciences, Chinese Academy of Medical Sciences and Peking Union Medical College, Beijing 100005, China. Email: jun_li@ibms.pumc.edu.cn*

Introduction

Skeletal muscle atrophy, characterized by decreased muscle mass and function, threatens the quality of life.[1] Muscle atrophy can occur as a result of physiological or pathological factors, such as ageing,[2,S1] immobilization[3] or diseases.[4,S2] Skeletal muscle is a heterogeneous tissue that consists of mononuclear muscle stem cells (satellite cells) and multinuclear myofibres.[5] Satellite cells, the multipotent stem cells that are responsible for skeletal muscle regeneration,[6,S3] activate and finally form terminally differentiated myofibres upon skeletal muscle injury to maintain muscle integrity.[7] Myofibre is the main cell type of skeletal muscle, and its size and quality determine muscle mass and function.[8] Weakened satellite cells' myogenic capacity and accelerated myofibre wasting are significant contributors of muscle atrophy.[9,S4,S5] Mitochondrial dysfunctions are important factors for impaired myogenic capacity of satellite cells,[10,S6] and excessive degradation of myofibrillar proteins, controlled by abnormal activation of the ubiquitin–proteasome and autophagy–lysosome pathways,[11,S7] is an important cause or feature of myofibre wasting.[12] Despite significant advances in understanding the mechanisms that regulate muscles loss in diseases, effective pharmacological treatments for atrophying muscle are currently unavailable, necessitating a new perspective of mechanistic insight. Recent studies reveal that common coordinators exist, which regulate functions of muscle cells at different developmental stages. For example, Ca^{2+} acts as a coordinator in both satellite cell myogenic differentiation and myotube maturation,[13] and palladin, a scaffolding microfilament-associated phosphoprotein, is reported to inhibit early myogenesis but promotes myotube maturation.[14] Discovering these coordinators might open a new avenue of combating muscle atrophy.

Deleted in breast cancer 1 (DBC1) is a large multidomain protein that regulates various cellular functions, including apoptosis, metabolism, tumourigenesis and DNA repair.[15,S8] Emerging evidences suggest that DBC1 may also play a role in regulating muscle functions. Studies have shown that DBC1 deletion mice are more susceptible to aortic dissections upon angiotensin II (ANG II), partially due to reduced activation of vascular smooth muscle cells in the arterial walls.[16] Additionally, DBC1 knockout mice also exhibit symptoms of experimental autoimmune myasthenia gravis (EAMG), such as severe limb weakness, presumably due to the inhibition of NF-κB pathway.[17] Moreover, DBC1 has been shown to inhibit sirtuin 1 (SIRT1) activity,[18] which has been linked to negative regulation of satellite cell differentiation.[19,S9] These findings suggest that DBC1 plays an important role in regulating muscle functions that have yet to be fully elucidated. Further research is necessary to clarify the specific roles of DBC1 in skeletal muscle.

Forkhead box O3 (FOXO3) is the main member of forkhead box O (FOXO) family that is expressed in muscles and plays a key regulator of atrophy.[20] FOXO3 induces the expression of atrophy-related ubiquitin ligases Atrogin1 and Murf1, which are the main factors of ubiquitin–proteasome pathway responsible for protein degradation and muscle loss.[11,S10] Additionally, FOXO3 activates the autophagy–lysosome pathway by inducing expression of autophagy-related genes, such as light chain 3 (LC3).[21] FOXO3 is also highly expressed in quiescent satellite cells and maintains their quiescence,[22,S11] and its absence hampers self-renewal of satellite cells, leading to myogenesis.[23,S12] However, the precise mechanism by which FOXO3 regulates myogenesis remains unclear.

In this study, we hypothesize that DBC1 plays a regulatory role in maintaining skeletal muscle integrity. Our findings reveal that DBC1 plays an essential role in enhancing myogenesis and repressing myofibre wasting. Specifically, we demonstrated that DBC1 negatively regulated FOXO3 protein homeostasis through mouse double minute 2 (MDM2)-mediated ubiquitination system. As a result, DBC1 deficiency led to increased FOXO3 protein levels, which impaired myogenic capacity of satellite cells by disrupting mitochondrial functions and led to myofibre wasting via activating ubiquitin–proteasome and autophagy–lysosome pathways. Our study suggests that DBC1 regulates myogenesis and myofibre maintenance via the MDM2/FOXO3 pathway, shedding light on the mechanisms underlying age-related muscle atrophy and offering potential new perspectives for combating skeletal muscle atrophy.

Methods

Cell culture

C2C12 cells (BMCR) were cultured in Dulbecco's modified Eagle's medium (Corning, 10-013-CVRC) containing 10% foetal bovine serum (FBS) (Gibco, 16140071) and 1% penicillin/streptomycin (Solarbio, P1400). For differentiation of C2C12 myoblasts into myotubes, cells were transferred to DMEM containing 2% horse serum (Thermo, 26050070) and then changing fresh medium every 2 days.

Mouse handling

All C57BL/6 mice were purchased from SPF Biotechnology (Beijing, China). Mice were housed in specific pathogen-free (SPF) barrier facilities. All procedures were approved by the Animal Ethics Committee of Peking Union Medical College. DBC1 knockdown mice were performed by intramuscular injection of 2.00 E + 11 vg of adeno-associated virus 9 (AAV9) (BrainVTA, Wuhan China) carrying single-guide RNA (sgRNA) against DBC1 or a scram-bled sgRNA control into hindlimb tibialis anterior (TA) muscles.

Grip force test

The muscle forces of DBC1 knockdown and control mice were evaluated by using a BIO-GS3 claw grip tester. Each mouse was tested for five times, and the data collected are the average of the three highest values out of the five tests.

Endurance test

Muscle endurance capacity was evaluated by using a flat motorized treadmill (ZH-PT/5S, Zhenghua Biology). The test started at a speed of 10 m/min, followed by 12, 15 and 18 m/min for 5 min and maintained at 20 m/min till the endpoint. The experiment ended when the mice stopped running and did not attempt to run again after being electrocuted more than 10 times.

Immunoblotting

Samples were homogenized in lysis buffer (50-mM tris, pH 7.5, 150-mM NaCl, 0.5% NP-40) supplemented withprotease inhibitor cocktail (MedChemExpress [MCE], HY-K0010), followed by SDS-PAGE and electrotransferred to 0.45-μm polyvinylidene difluoride (PVDF) membrane (Millipore). Membranes were blocked with 5% non-fat dry milk in tris-buffered saline with Tween 20 (TBST) for 1 h and then incubated with primary antibodies overnight at 4°C, followed by incubation with proper secondary antibodies. Antibodies were used at the following concentrations: anti-DBC1 (1:2000, Bethyl, A300434A), anti-myogenin (MyoG) (1:500, Santa Cruz, sc-52903), anti-myosin heavy chain (MHC) (1:1000, Developmental Studies Hybridoma Bank [DSHB], MF20-C), anti-FOXO3 (1:2000, Cell Signaling Technology [CST], 2497S), anti-Atrogin1 (1:500, Santa Cruz, sc-16806), anti-Murf1 (1:500, Santa Cruz, sc-398608), anti-LC3 (1:500, ABclonal, A19665), anti-MDM2 (1:500, Santa Cruz, sc-13161), anti-ubiquitin (1:500, Santa Cruz, sc-8017), anti-β-tubulin (1:5000, CMCTAG, AT0003) and anti-GAPDH (1:5000, Millipore, mab374). Blotting signals were visualized on Azure 200 Gel Imager (Azure Biosystems).

Immunofluorescence

Muscle sections (10 μm) were fixed with 4% polyformaldehyde for 30 min, followed by three times of washing in phosphate-buffered saline (PBS). The samples were permeabilized using PBS containing 0.5% Triton X-100 for 15 min and then blocked with 1% bovine serum albumin for 2 h. The samples were incubated with anti-MyoG (1:100, Santa Cruz, sc-52903), MHC (1:100, DSHB, MF20-C), Ki-67 (1:500, Abcam, ab15580), anti-DBC1 (1:200, Absin, abs117680) or anti-FOXO3 (1:200, Absin, abs115009) overnight at 4°C. The samples were washed with PBS containing 0.05% Tween 20 for three times and then incubated with the secondary antibodies (Alexa Fluor® 568 and 488 antibodies, 1:500, Abcam) for 50 min in the dark. Nuclei were counterstained with 4′,6-diamidino-2-phenylindole (DAPI), and images were taken using Lecia DM6 B Upright Microscope.

Mitochondrial membrane potential assay

Tetramethylrhodamine methyl ester perchlorate (TMRM, Sigma, T5428) was diluted with serum-free medium at the final concentration of 20 nM. The medium was removed and replaced with 500-μL diluted TMRM, using 10-μM carbonyl cyanide 4-(trifluoromethoxy)phenylhydrazone (FCCP, MCE, 370-86-5) as positive control, and then cells were incubated at 37°C for 20 min. After incubation, cells were washed three times and resuspended in PBS. Fluorescein isothiocyanate (FITC) channel was selected for flow cytometry detection.

Reactive oxygen species measurement

Dichlorodihydrofluorescein diacetate (DCFH-DA) (Beyotime, S0033S) was diluted with serum-free medium at the final concentration of 10 μM. The medium was removed and replaced with 500-μL diluted DCFH-DA, using 10-μM rotenone (MCE, HY-B1756) as positive control, and then cells were incubated at 37°C for 20 min. After incubation, cells were washed three times and resuspended in PBS. FITC channel was selected for flow cytometry detection.

Mitochondria number

MitoTracker Red CMXRos (Beyotime, C1049B) was diluted with serum-free medium at the final concentration of 100 nM. The medium was removed and replaced with 500-μL diluted MitoTracker Red CMXRos, and then cells were incubated at 37°C for 20 min. After incubation, cells were washed three times and resuspended in PBS. FITC channel was selected for flow cytometry detection.

Succinate dehydrogenase and glycerophosphate dehydrogenase staining

For succinate dehydrogenase (SDH) staining, the myotubes or muscle sections (10 μm) were incubated in a solution consisting of 1-mM sodium azide, 1-mM L-methoxyphenazine methosulfate (MPMS, Macklin, M860955), 1.5-mM nitroblue tetrazolium (NBT) (Macklin, N814596), 5-mM EDTA and 100-

mM sodium phosphate buffer (pH 7.6) in the dark at 37°C for 10 min, followed by incubation in a substrate solution consisting of 48-mM succinic acid (Macklin, L897377) for 5–10 min. For glycerophosphate dehydrogenase (GPDH) staining, the myotubes or muscle sections (14 μm) were incubated with a solution consisting of 1-mM sodium azide, 1-mM MPMS, 1.2-mM NBT and 100-mM sodium phosphate buffer (pH 7.4) at 37°C for 20 min, followed by another incubation with a substrate solution consisting of 9.3-mM α-glycerophosphate (Sigma, G9422) for 10–20 min. The images were captured using Lecia DM6 B Upright Microscope.

Haematoxylin and eosin staining

Frozen tissue blocks used for haematoxylin and eosin (H&E) staining were sectioned at 10 μm. H&E staining was conducted by Wuhan Servicebio Technology Company following standard protocol. Images were taken by Leica DM6 B Upright Microscope.

Mitochondrial bioenergetic measurements

The cells were plated in an XF 24-well microplate (Seahorse Bioscience) at a density of 20 000 cells per well and differentiated for 2 days. Oxygen consumption rate was measured in cells at 37°C using an XF24 analyser (Seahorse Bioscience) according to manufacturer's instructions; 10-μM oligomycin (MCE, 1404-19-9), 40-μM FCCP and 10-μM rotenone (MCE, HY-B1756)/antimycin (Sigma, A8674) were used to detect the uncoupled respiration, maximal respiration and nonmitochondrial respiration, respectively.

Statistical analysis

Data were expressed as mean ± standard deviation. *P* values were calculated in GraphPad Prism using two-tailed Student's *t* test or one-way analysis of variance (ANOVA) for multiple comparison. *P* values are denoted in figures as follows: ns (not significant), $^{*}P < 0.05$, $^{**}P < 0.01$, $^{***}P < 0.001$ and $^{****}P < 0.0001$.

Results

The deficiency of DBC1 is associated with muscle atrophy and impaired muscle regeneration

In atrophic skeletal muscle of old mice (*Figure 1A*), mice with limb immobilization (*Figure 1B*) and cachexia mice (*Figure S1a–c*), a significant reduction in DBC1 protein levels was observed, suggesting a potential role of DBC1 in muscle atrophy. To investigate this further, we created TA muscle-specific DBC1 knockdown mice by intramuscularly injecting adeno-associated virus (AAV9) particles delivering sgRNA for DBC1 or scrambled control into TA muscles of 3-month-old C57BL/6 mice (*Figure 1C*). Two months after virus injection, DBC1 was significantly reduced (*Figure S1d*), whereas DBC1 knockdown had no effect on body weight of mice (*Figure S1e*). In DBC1 knockdown mice, the grip force and endurance of muscles were significantly decreased (*Figure 1C*); the loss of muscle mass was greater as also evidenced by smaller calf girth (*Figure 1D*). Consistently, after DBC1 knockdown in TA muscles, the myofibre cross-sectional areas (CSAs) were also significantly reduced (*Figure 1E*), suggesting shrinkage of myofibres. These data indicate that lacking DBC1 in TA muscles causes muscle atrophy. Considering that dysfunctional myogenetic capacity of satellite cells also contributes to muscle atrophy,[24] we wondered whether DBC1 knockdown affects myogenesis. We introduced cardiotoxin (CTX)-mediated injury in TA muscles of control and DBC1 knockdown mice (*Figure 1F*). Ten days after injury, TA muscle mass remained remarkedly reduced in DBC1 knockdown mice (*Figure S2a–c*). The CSAs of myofibres with centralized nuclei were significantly decreased, where the fluorescence signals of MyoD or MyoG were detected (*Figures 1F* and *S2d,e*). At all, these results indicate that DBC1 knockdown results in muscle atrophy and hinders muscle regeneration.

DBC1 modulates myogenesis

To further investigate the involvement of DBC1 in myogenesis, we utilized C2C12 cells as an in vitro myoblast model. *DBC1* mRNA expression was found to increase during C2C12 cell differentiation in a similar pattern to *MyoG*, the early marker of myogenesis (*Figure 2A*). The increased expression of DBC1 during myogenesis was confirmed by immunofluorescence staining, which revealed a greater abundance of DBC1 proteins on the second day of differentiation (D2) (*Figure 2A*). To verify this in vivo, we injured TA muscles of the wild-type mice with intramuscular CTX injection (*Figure S3a*) and co-stained DBC1 with markers for different types of muscle cells. The results showed that DBC1 protein levels were significantly increased 5 days after injury in 92.5% of $MyoG^{+}$ cells, which represent stem cell-derived myoblasts, and 95.6% of central nuclei of MHC^{+} cells, which represent newly formed myofibres (*Figure 2B*), but not in the satellite cells, as indicated by the unchanged ratio of $DBC1^{+}/Pax7^{+}$ cells and $Pax7^{+}$ cells (*Figure S3b*). These results imply that the increase of DBC1 proteins occurs only during myogenesis. Consistently, knockdown of DBC1 in C2C12 cells led to a significant inhibition of myogenesis, as evidenced by reduced MyoG and MHC protein levels (*Figure 2C*) and decreased percentages of $MyoG^{+}$ nuclei (*Figure 2D*), as well as reduced fusion index (*Figure 2E*). RNA-sequencing analysis of DBC1

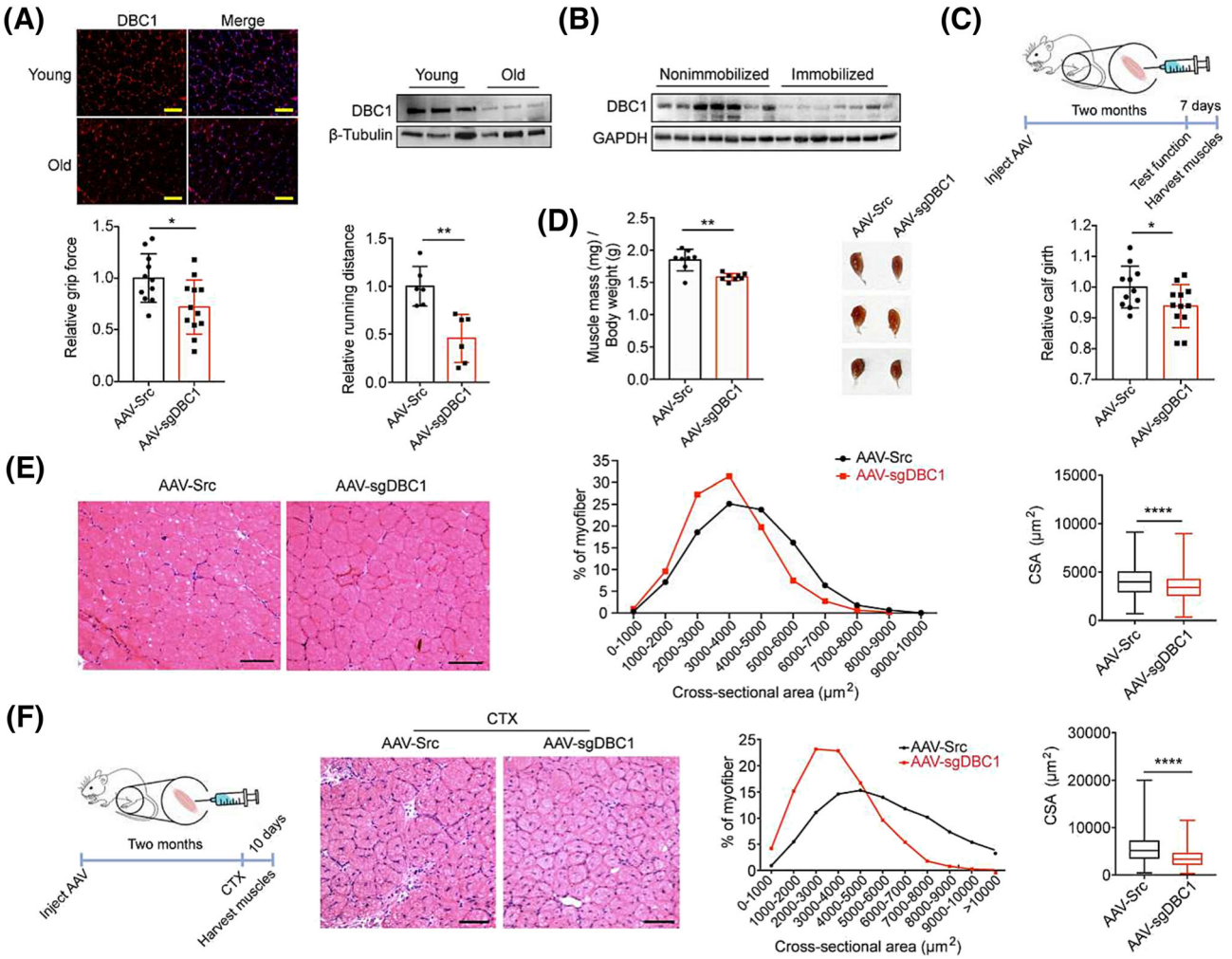

Figure 1 DBC1 deletion impairs skeletal muscle integrity and regeneration. (A) Immunofluorescence staining (left) and western blotting analysis (right) for DBC1 protein levels in TA muscles isolated from young (3 months) and old (24 months) mice. Nuclei were counterstained with DAPI (blue). Scale bars = 100 μm. (B) Western blotting analysis for DBC1 protein levels in TA muscles isolated from C57BL/6J mice with limbs immobilized for 3 weeks. (C) Schematic to illustrate experimental design of knocking down DBC1 in mouse TA muscles: TA muscles of 8-week-old male C57BL/6J mice were injected intramuscularly with AAV-sgDBC1 or AAV-src. Relative grip force and relative running distance (relative to those of AAV-src control group) were tested 2 months after the injection, followed by collecting muscle samples 7 days later (n = 12 for each group). (D) TA muscles weight, normalized to body weight (n = 8 for each group) (left), representative images of TA muscles (middle) and relative calf girth (n = 12 for each group) (right) of DBC1 knockdown and control mice. (E) (left) Representative images of haematoxylin and eosin (H&E) staining of TA muscles isolated from DBC1 knockdown and control mice. Scale bar = 100 μm. (right) Percentage distribution of myofibre cross-sectional area (CSA) (middle) and the mean CSA (right) in TA muscles of DBC1 knockdown and control mice calculated from the H&E staining sections was quantified. Data were pooled from 2502 myofibres for control mice and 3285 myofibres for DBC1 knockdown mice (four mice for each group). (F) (left) Schematic to illustrate regeneration of TA muscles in DBC1 knockdown mice: TA muscles from 8-week-old C57BL/6J mice were injected intramuscularly with AAV-sgDBC1 or AAV-src for 2 months to knock down DBC1 and then were damaged by injecting 50-μL cardiotoxin (CTX, 10 μM), intramuscularly. Muscle samples were collected 10 days after CTX injection. (right) Representative images of H&E staining of TA muscles isolated from DBC1 knockdown or control mice 10 days after CTX-induced damage. Percentage distribution of CSA and mean CSA of regenerating myofibres with central nuclei, calculated from the H&E staining sections, was quantified. Data were pooled from 4392 myofibres for control mice and 5850 myofibres for DBC1 knockdown mice (four mice for each group). All P values were calculated using two-tailed Student's t test.

knockdown C2C12 cells further confirmed the necessity of DBC1 in myogenesis. We identified 3936 genes whose expression was significantly modulated after DBC1 knockdown, of which 2101 were downregulated (*Figure S4*). Gene Ontology (GO) analysis of these downregulated genes revealed enrichment in skeletal muscle cell differentiation and skeletal muscle development pathways (*Figure 2F*), which further demonstrates the importance of DBC1 for myogenesis. DBC1 was reported to affect cell cycle and apoptosis.[15] Notably, we ruled out the possibility that the impaired

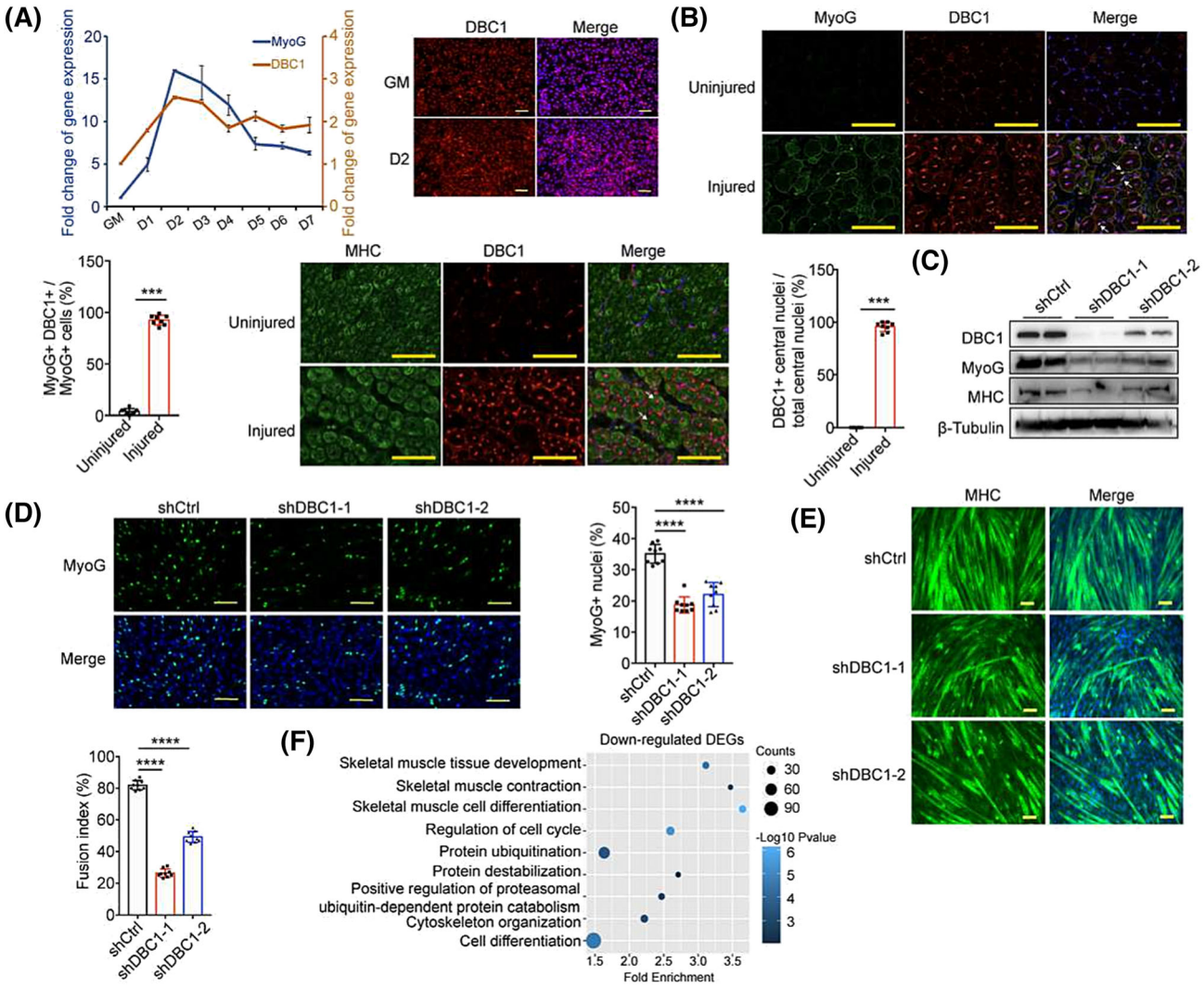

Figure 2 DBC1 regulates myogenesis. (A) (left) Time-course gene expression of *DBC1* and *MyoG* in proliferating and differentiating C2C12 cells, determined by RT-qPCR. GM represents proliferating stage. D1, D2, D3, D4, D5, D6 and D7 represent a differentiating time of 1, 2, 3, 4, 5, 6 or 7 days, respectively. (right) Immunofluorescence staining of DBC1 (red) in proliferating C2C12 cells (GM) and C2C12 cells that had been induced to differentiate for 2 days (D2). Nuclei were counterstained with DAPI (blue). Scale bars = 100 μm. (B) Immunofluorescence staining of MyoG (green) and DBC1 (red) as well as MHC (green) and DBC1 (red) in TA muscles that were damaged by CTX for 5 days (injured) or not (uninjured). Nuclei were counterstained with DAPI (blue). Arrowheads indicate representative cells express DBC1 and MyoG meanwhile or central nuclei express DBC1. Scale bars = 100 μm. The percentages of DBC1-expressing MyoG$^+$ myoblasts measured by the ratio of MyoG$^+$/DBC1$^+$ cells compared to MyoG$^+$ myoblasts. Percentages of DBC1-expressing central nuclei measured by the ratio of DBC1$^+$ central nuclei compared to total central nuclei. (C) Western blotting analysis for DBC1, MyoG and MHC protein levels in DBC1 knockdown and control C2C12 cells that had been induced to differentiate for 2 days. (D) (left) Immunofluorescence staining of MyoG (green) in DBC1 knockdown and control C2C12 cells that had been induced to differentiate for 2 days. Nuclei were counterstained with DAPI (blue). Scale bars = 100 μm. (right) The proportion of MyoG$^+$ nuclei was quantified. (E) Immunofluorescence staining of MHC (green) and quantification of the fusion index in DBC1 knockdown and control C2C12 cells that had been induced to differentiate for 7 days. Nuclei were counterstained with DAPI (blue). Scale bars = 100 μm. (F) Gene Ontology (GO) analysis of the downregulated genes in DBC1 knockdown C2C12 cells, performed with $-\log_{10}$ (*P* value) plotted as a function of classification meeting a *P* value of <0.05. *P* values were calculated using two-tailed Student's *t* test (B) or one-way ANOVA for multiple comparison (D, E).

myogenesis in DBC1 knockdown cells was due to changes in cell proliferation or apoptosis, as there were no changes in proliferation rate or percentages of apoptotic cells observed (*Figure S5*). Overall, these results provide compelling evidence that DBC1 plays an indispensable role in myogenesis.

DBC1 knockdown results in myotube wasting

Myofibre shrinkage, which is a characteristic of muscle atrophy,[25] was observed in skeletal muscle of DBC1 knockdown mice (*Figure 1E*), raising the possibility that DBC1 may affect myofibre wasting. To investigate this, we again

DOI: 10.1002/jcsm.13398

knocked down DBC1 in fully differentiated myotubes (*Figure S6a*) and observed similar results to those in vivo, with the myotubes becoming shorter in length and thinner in diameter (*Figure 3A*). Dexamethasone (DEX) and serum fast are known to induce muscle atrophy,[26] and in these cases, DBC1 protein level decreased (*Figures 3B* and *S6b*), while overexpression of DBC1 improved the DEX and serum fast induced myotube wasting to some extent (*Figures 3C* and *S6c,d*). Consistently, DBC1 overexpression in old mice and mice with limb immobilization also significantly suppressed muscle atrophy (*Figure S6e,f*). Along with atrophy, the metabolism of myofibres declined.[27] DBC1 knockdown led to significant reductions in the expression of metabolic genes, especially those related to glycolysis such as *HK2* and *Pfkm* (*Figure 3D*). Histochemical staining showed that enzymatic activities of α-GPDH and SDH decreased in DBC1 knockdown myotubes as well (*Figure 3E*). Similar decreases were observed in the TA muscles with DBC1 deletion (*Figure 3F*). Collectively, these findings suggest that DBC1 is likely involved in suppressing myofibre wasting.

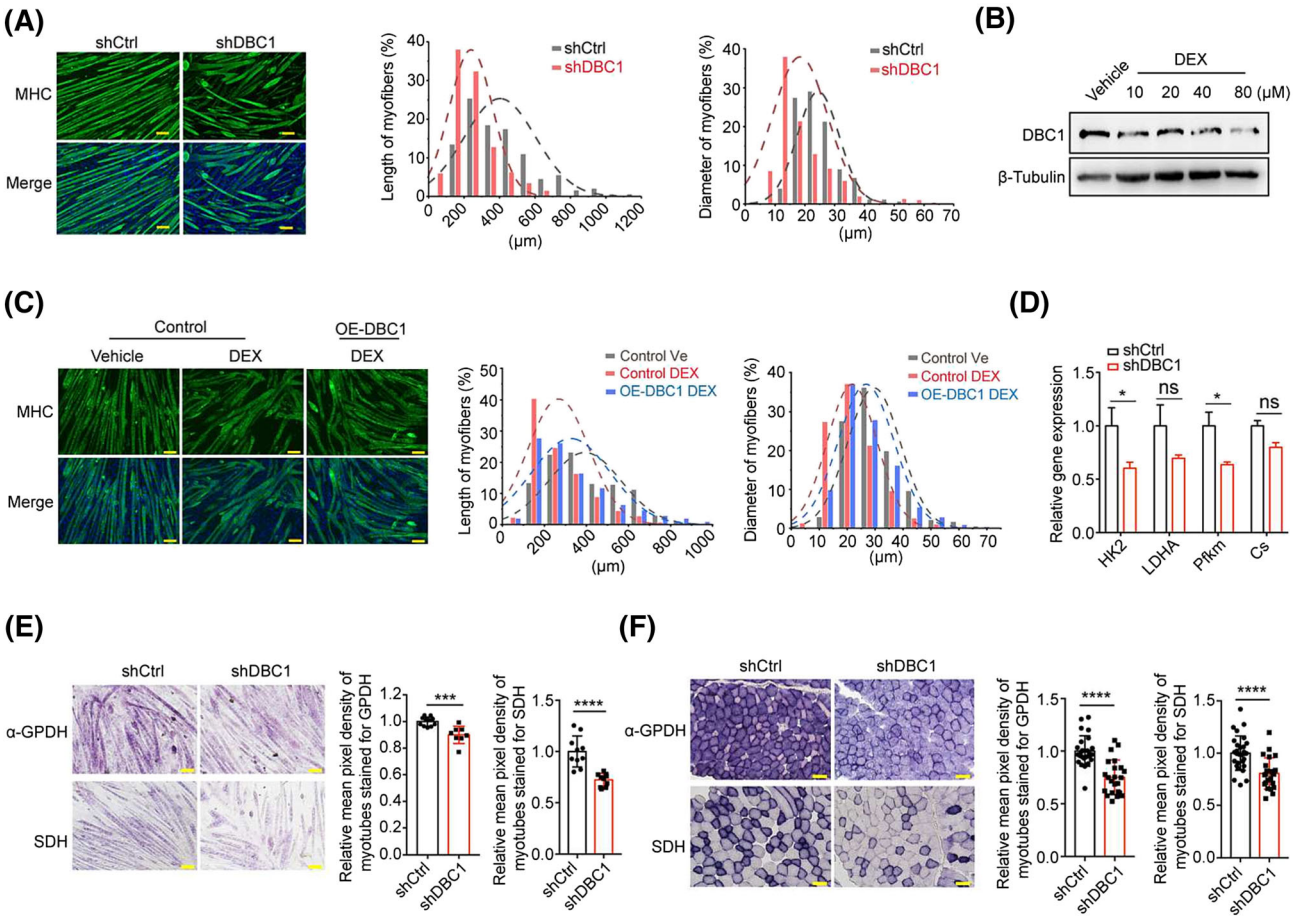

Figure 3 Lacking DBC1 accelerates myofibre loss. (A) (left) Immunofluorescence staining of MHC (green) in myotubes with DBC1 knockdown. (right) Percentage distribution of length and diameter of myotubes was quantified. C2C12 cells were induced to fully differentiate for 7 days and then were added with lentivirus to knock down DBC1 for 2 days, and then MHC was immunostained after knocking down DBC1, with nuclei counterstained by DAPI (blue). Scale bar = 100 μm. (B) Western blotting analysis for DBC1 protein levels in myotubes (fully differentiated for 7 days) that were treated with dexamethasone (DEX) at the dose of 10, 20, 40 or 80 μM, respectively, for 24 h. (C) (left) Immunofluorescence staining of MHC (green) in control myotubes, DEX-treated control myotubes and DEX-treated DBC1-overexpressing myotubes, with nuclei counterstained by DAPI (blue). (right) Percentage distribution of the length and diameter of myotubes. C2C12 cells were induced to fully differentiate for 5 days before being infected with the control retrovirus or the retrovirus overexpressing DBC1 for 48 h. After DBC1 was overexpressed, DEX (80 μM) was added for 24 h. Scale bar = 100 μm. (D) Relative gene expression of *HK2*, *LDHA*, *Pfkm* and *Cs* in DBC1 knockdown or control myotubes; the procedure of treating myotubes was same as described in (A). (E) (left) Representative histochemical staining for α-GPDH and SDH enzymatic activities in DBC1 knockdown myotubes. (right) Quantification of mean pixel density of myotubes stained for α-GPDH and SDH. (F) (left) Representative histochemical staining for α-GPDH and SDH enzymatic activities in the TA muscles of DBC1 knockdown mice. (right) Quantification of mean pixel density of myofibres stained for α-GPDH and SDH. All *P* values were calculated using two-tailed Student's *t* test.

DOI: 10.1002/jcsm.13398

DBC1 regulates myogenesis and myofibre homeostasis by suppressing FOXO3

To understand how DBC1 regulates myogenesis and myofibre homeostasis, we investigated the potential involvement of SIRT1, as DBC1 inhibits SIRT1 activity,[28] which inhibits myogenesis.[19] However, treatment with SIRT1 inhibitor Ex-527 (*Figure S7a*,*b*) or knockdown of SIRT1 (*Figure S7c–e*) in DBC1 knockdown C2C12 cells failed to rescue the bad differentiation, as confirmed by non-significant increase of the percentages of MyoG$^+$ nuclei and the fusion index, indicating that DBC1's effect on myogenesis was not dependent on SIRT1.

FOXO3, whose expression remarkably decreased upon satellite cells entering myogenic process, was reported to inhibit myogenesis.[22] In differentiating C2C12 cells, we observed a dramatic decrease in FOXO3 protein levels compared to the proliferating cells, which disappeared in DBC1 knockdown cells (*Figure 4A*). Knocking down DBC1 increased FOXO3 levels during myogenesis (*Figure 4A*), and overexpressing DBC1 reversed the increase (*Figure S8a*). Consistently, FOXO3 levels were higher in CTX-injured TA muscles isolated from DBC1 knockdown mice (*Figure 4B*). In contrast, knocking down DBC1 in proliferating C2C12 cells had no effect on FOXO3 protein levels (*Figure S8b*). These data indicated a negative correlation between DBC1 and FOXO3 protein levels during myogenesis. Meanwhile, knocking down FOXO3 in DBC1 knockdown C2C12 cells significantly increased the percentages of MyoG$^+$ nuclei and MyoG protein level (*Figures 4C* and *S9a*,*b*), as well as cell fusion rates and MHC protein levels (*Figures 4D* and *S9c*). These results suggest that DBC1 regulates myogenesis by suppressing FOXO3. In addition to inhibiting myogenesis, FOXO3 was also reported to control myofibre wasting.[21] In the muscles of aged mice, DBC1 protein decreased compared to those of the young (*Figure 1A*), while FOXO3 protein levels increased (*Figure S10*). These data suggest that the negative correlation in DBC1 and FOXO3 proteins also exists in mature myofibres and that DBC1 might suppress myofibre wasting by inhibiting FOXO3. Consistent with this hypothesis, overexpressing DBC1 in fully differentiated myotubes decreased FOXO3 protein levels (*Figure 4E*) and improved myotube quality as indicated by the stronger myotubes (*Figure 4F*). These results indicate that DBC1 facilitates myogenesis and prevents myotube wasting by negatively regulating FOXO3.

DBC1 deletion impairs mitochondrial functions due to increased FOXO3 during myogenesis

After demonstrating that DBC1 regulates myogenesis via suppressing FOXO3 (*Figure 4C*,*D*), the question of how FOXO3 inhibits this process remains unanswered. FOXO3 has been reported to suppress mitochondrial functions.[29] Mitochondria are linked to many factors that dictate the fate of satellite cells including metabolic reprograming upon activation,[30] self-renewal and differentiation.[S13,S14] We hypothesized that DBC1 controlled myogenesis through FOXO3-mediated regulation of mitochondrial functions. DBC1 knockdown reduced basal respiration, ATP production and maximal respiration of differentiating C2C12 cells measured by the Seahorse mitochondria stress test, while silencing FOXO3 in DBC1 knockdown cells reversed these declines (*Figure 5A*). Consistent with the reduced mitochondrial respiratory function, mitochondrial membrane potential and reactive oxygen species (ROS) production were also decreased in differentiating DBC1 knockdown C2C12 cells, which could be rescued by silencing FOXO3 (*Figure 5B*,*C*). The possibility that FOXO3 impairs mitochondrial function by decreasing the number of mitochondria was ruled out, as no difference was observed after knocking down FOXO3 in differentiating DBC1 knockdown C2C12 cells (*Figure 5D*). However, no statistic difference was observed in mitochondrial membrane potential, mitochondria number, and ATP and ROS production in proliferating DBC1 knockdown C2C12 cells compared to the control cells (*Figure S11*). These results support the notion that elevated FOXO3 levels due to DBC1 deficiency hamper myogenesis through repressing mitochondrial functions.

DBC1 knockdown accelerates myofibre wasting via FOXO3-mediated ubiquitin–proteasome and autophagy–lysosome pathways

Next, we investigated how DBC1 regulated myofibre wasting. Given that FOXO3 regulates muscle atrophy by activating ubiquitin–proteasome pathway and autophagy–lysosome pathway,[11] we first examined the expressions of Atrogin1 and Murf1, muscle-specific ubiquitin ligases of ubiquitin–proteasome pathway, in DBC1 knockdown myotubes. We found that both Atrogin1 and Murf1 were upregulated at transcriptional and protein levels in DBC1 knockdown myotubes (*Figure 6A*), along with significantly increased proteasome activity (*Figure 6B*), suggesting activation of ubiquitin–proteasome pathway. Autophagy–lysosome pathway was also activated in DBC1 knockdown myotubes, as evidenced by increased conversion of LC3-I to LC3-II (*Figure 6C*). This was confirmed by increased yellow puncta in DBC1 knockdown myotubes transfected with a fluorescent reporter plasmid to visualize autophagosomes (*Figure 6C*). Consistently, we also found increased FOXO3 protein in mouse skeletal muscle with DBC1 ablation (*Figure 6D*), as well as increased Atrogin1 and Murf1 and the conversion of LC3-I to LC3-II (*Figure 6E*). Treating DBC1 knockdown myotubes with carbenoxolone, an inhibitor blocking FOXO3's transcriptional activity,[31] decreased mRNA levels of *Atrogin1* and *Murf1* (*Figure S12a*) and improved the quality of myotubes (*Figure 6F*). Autophagy inhibitor bafilomycin A1 and proteasome inhibitor MG-132 achieved similar rescue effects on the quality of myotubes with DBC1 ablation (*Figure 6F*). FOXO3 nuclear

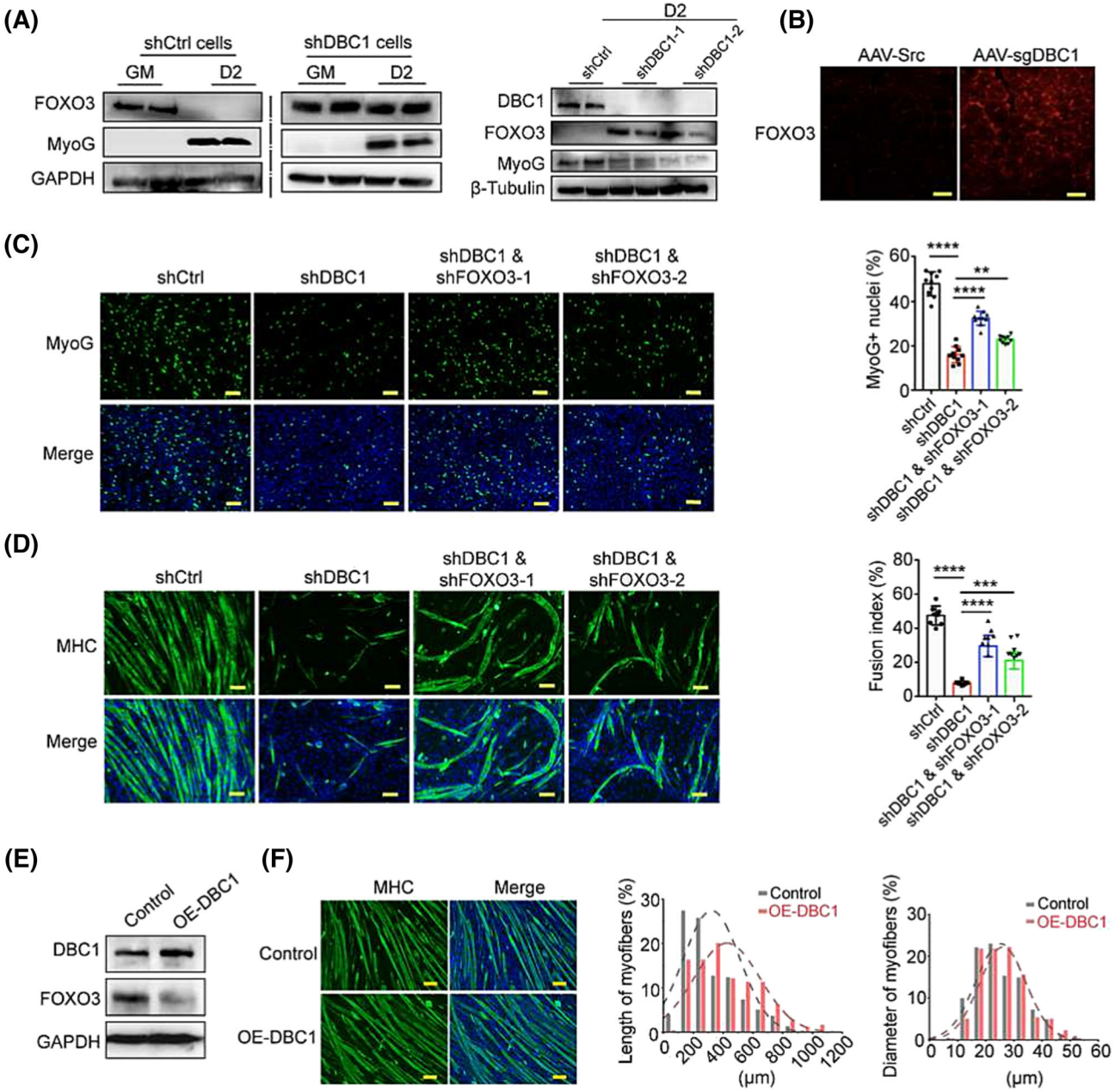

Figure 4 DBC1 governs myogenesis and myotube maintenance by suppressing FOXO3 protein levels. (A) (left) Western blotting analysis for FOXO3 and MyoG protein levels in proliferating (GM) and differentiating (differentiate for 2 days [D2]) control C2C12 cells or DBC1 knockdown C2C12 cells. (right) Western blotting analysis for FOXO3 and MyoG protein levels in DBC1 knockdown or control C2C12 cells that had been induced to differentiate for 2 days (D2). (B) Immunofluorescence staining of FOXO3 (red) in DBC1 knockdown TA muscles of mice that were damaged by CTX, as described in *Figure 1*. Nuclei were counterstained with DAPI (blue). Scale bars = 100 μm. (C) (left) Immunofluorescence staining of MyoG (green) in DBC1 knockdown, DBC1 and FOXO3 double knockdown or control C2C12 cells that had been induced to differentiate for 2 days. Nuclei were counterstained with DAPI (blue). Scale bars = 100 μm. (right) Quantification of the proportion of $MyoG^{+}$ nuclei. (D) (left) Immunofluorescence staining of MHC (green) in DBC1 knockdown, DBC1 and FOXO3 double knockdown or control C2C12 cells that had been induced to differentiate for 7 days. Nuclei were counterstained with DAPI (blue). Scale bars = 100 μm. (right) Quantification of the fusion index. (E) Western blotting analysis for FOXO3 protein levels in myotubes after DBC1 overexpression. Before subjected to western blotting, the myotubes had been induced to differentiate for 7 days followed by infection of retrovirus to overexpress DBC1 for 2 days. (F) (left) Immunofluorescence staining of MHC (green) in DBC1 overexpression myotubes and control myotubes as described in (E). Nuclei were counterstained with DAPI (blue). Scale bar = 100 μm. (right) Quantification of myotube length and diameter. *P* values were calculated using one-way ANOVA for multiple comparison (C, D).

DOI: 10.1002/jcsm.13398

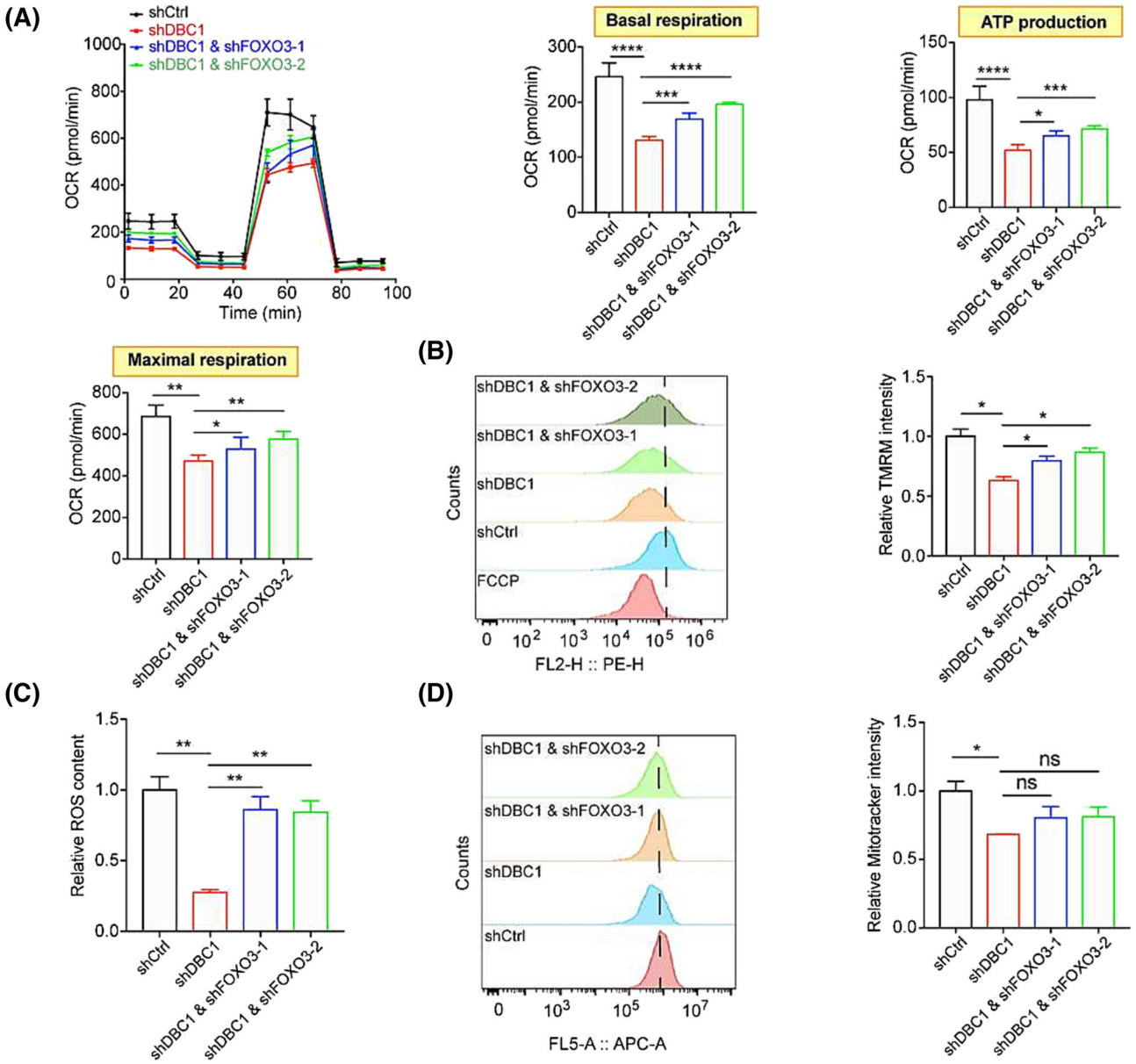

Figure 5 FOXO3 inhibits myogenesis by impairing mitochondrial functions. (A) Oxygen consumption rate (OCR) of DBC1 knockdown C2C12 cells, DBC1 and FOXO3 double knockdown C2C12 cells and the control cells that had been induced to differentiate for 2 days was performed to obtain bioenergetic parameters including basal respiration capacity, ATP-linked OCR and maximal respiration, in the presence of oligomycin (Oligo) (10 μM), FCCP (40 μM), antimycin A (10 μM) and rotenone (10 μM), analysed by an extracellular flux analyser (Seahorse Bioscience). (B) (left) Mitochondrial membrane potential (MMP) of DBC1 knockdown C2C12 cells, DBC1 and FOXO3 double knockdown C2C12 cells and the control cells that had been induced to differentiate for 2 days, analysed by FACS. (right) Quantification of the MMP. (C) Measurements of ROS production of DBC1 knockdown C2C12 cells, DBC1 and FOXO3 double knockdown C2C12 cells and the control cells that had been induced to differentiate for 2 days, analysed by FACS. (D) (left) The number of mitochondria in DBC1 knockdown C2C12 cells, DBC1 and FOXO3 double knockdown C2C12 cells and the control cells that had been induced to differentiate for 2 days, analysed by FACS. (right) Quantification of the number of mitochondria. All *P* values were calculated using one-way ANOVA for multiple comparison.

relocation is required for its transcriptional control of *Atrogin1* and *Murf1*, which is activated by FOXO3 dephosphorylation.[S15] In line with the inhibitory effect of DBC1 on muscle atrophy, we found that DBC1 knockdown considerably increased dephosphorylation of FOXO3 during differentiated status and DBC1 overexpression did the opposite (*Figure S12b,c*). However, in the proliferating stage, phosphorylated FOXO3 increased, causing more FOXO3 relocated to cytoplasm (*Figure S13*). Together, these results support that DBC1 suppresses myotube wasting via FOXO3-mediated activation of ubiquitin–proteasome and autophagy–lysosome pathways.

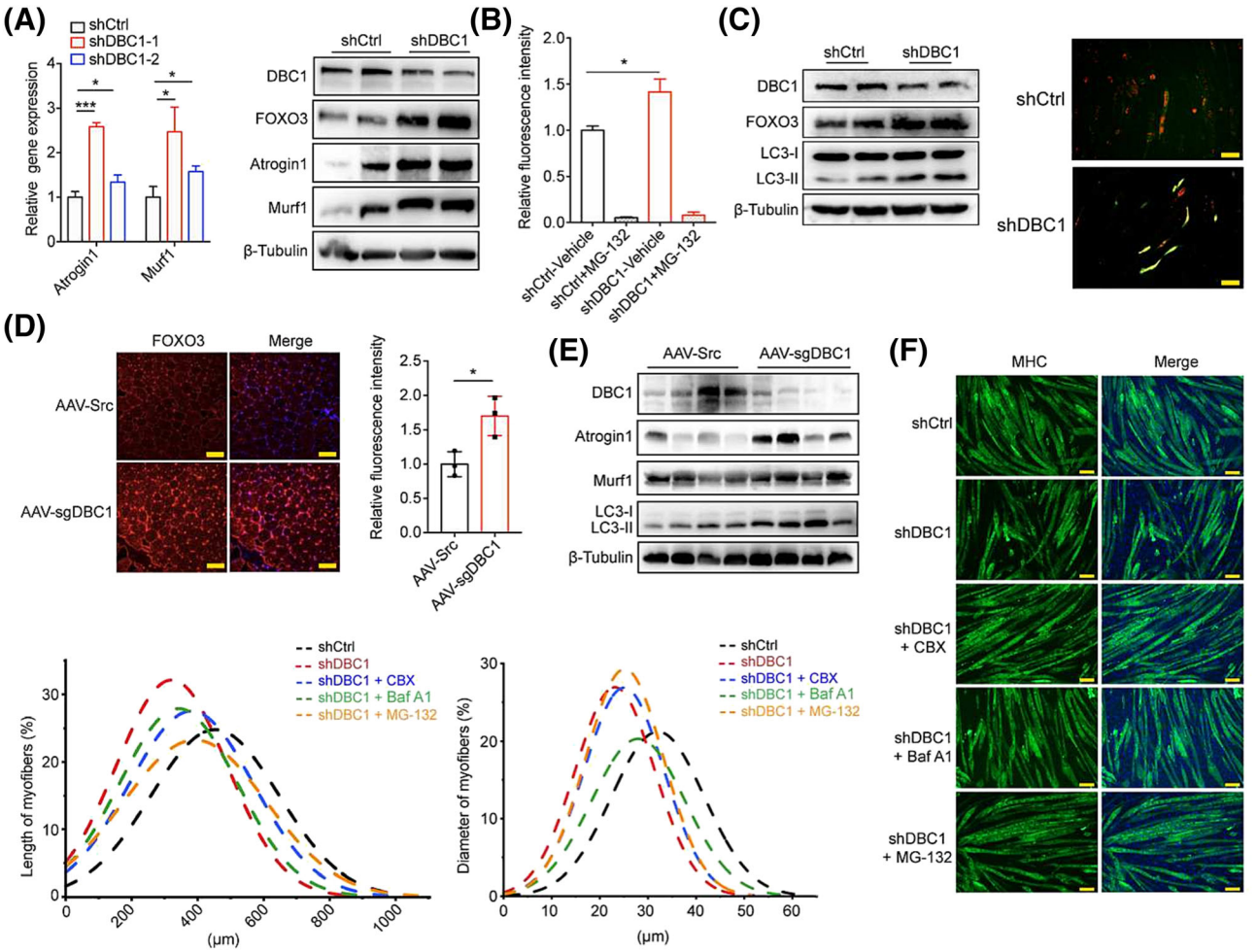

Figure 6 DBC1 knockdown accelerates myofibre wasting via FOXO3-mediated activation of ubiquitin–proteasome pathway and autophagy–lysosome pathway. (A) (left) Relative gene expression of *Atrogin1* and *Murf1* in DBC1 knockdown and control myotubes, determined by RT-qPCR. (right) Western blotting analysis for FOXO3, Atrogin1 and Murf1 protein levels in DBC1 knockdown and control myotubes. Before subjected to test, the myotubes had been induced to differentiate for 7 days followed by infection of lentivirus to knock down DBC1 for 2 days. (B) Proteasome activity in DBC1 knockdown or control myotubes. Proteasome activity was accessed in vitro using cell lysates of DBC1 knockdown and control myotubes that were treated as described in (A). MG-132 (20 μM) was added in assay as a negative control. (C) (left) Western blotting analysis for FOXO3, LC3-I and LC3-II protein levels in DBC1 knockdown and control myotubes that were treated as described in (A). (right) Representative images of DBC1 knockdown and control myotubes transfected with autophagy reporter plasmid are shown on the right. Scale bar = 100 μm. (D) (left) Immunofluorescence staining of FOXO3 (red) in DBC1 knockdown TA muscles of mice as described in *Figure 1C*. Nuclei were counterstained with DAPI (blue). Scale bars = 100 μm. (right) Quantification of fluorescence intensity (four mice for each group). (E) Western blotting analysis for Atrogin1, Murf1, LC3-I and LC3-II protein levels in TA muscles of DBC1 knockdown mice as described in *Figure 1C*. (F) Immunofluorescence staining of MHC (green) in control myotubes, DBC1 knockdown myotubes and DBC1 knockdown myotubes treated by carbenoxolone (CBX, 100 μM), bafilomycin A1 (0.5 nM) and MG-132 (10 nM), respectively. Nuclei were counterstained with DAPI (blue). Scale bar = 100 μm. And the myotube length and diameter were shown. *P* values were calculated using one-way ANOVA for multiple comparison (A, B).

DBC1 negatively regulates FOXO3 via ubiquitination–proteasome pathway

To further investigate how DBC1 modulates FOXO3, we first tested the mRNA expression of *FOXO3* but found that its transcription was not affected by DBC1 deletion in both proliferating and differentiating C2C12 cells (*Figure 7A*). The GO analysis of the downregulated genes in DBC1 knockdown C2C12 cells revealed a significant enrichment of protein ubiquitination and protein destabilization (*Figure 7B*), enlightening the possibility of FOXO3 degradation via ubiquitination upon differentiation. Previous studies reported that FOXO3 was subjected to MDM2-mediated ubiquitination and proteasome degradation and that MDM2 knockdown raised FOXO3 protein levels.[32,S16] We found that MDM2 protein was decreased after DBC1 knockdown in C2C12 cells (*Figures 7B* and *S14*). Treatment of MDM2 inhibitor Nutlin-3, or proteasome inhibitor MG-132 and leupeptin blocked the reduction of FOXO3 during differentiation (*Figures 7C* and *S15*), and the endogenously immunoprecipitated FOXO3

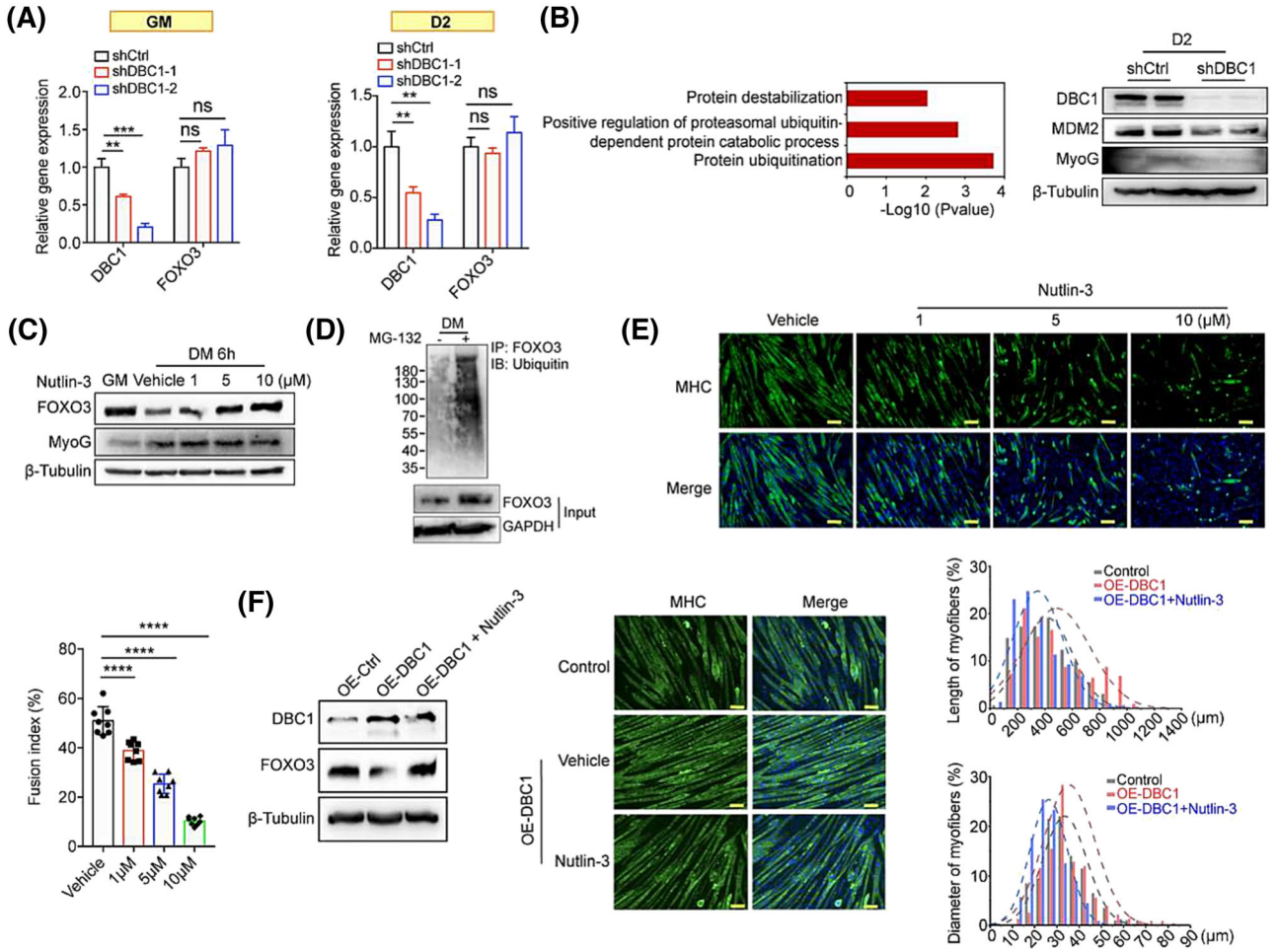

Figure 7 DBC1 promotes FOXO3 degradation via the ubiquitin–proteasome system. (A) Relative gene expression of *FOXO3* in proliferating (GM) (left) and differentiating (differentiate for 2 days [D2]) (right) DBC1 knockdown C2C12 cells and control cells, determined by RT-qPCR. (B) (left) Gene Ontology (GO) analysis of the downregulated genes in DBC1 knockdown C2C12 cells, performed with $-\log_{10}$ (*P* value) plotted as a function of classification meeting a *P* value of <0.05. (right) Western blotting analysis for MDM2 and MyoG protein levels in DBC1 knockdown or control C2C12 cells that had been induced to differentiate for 2 days (D2). (C) Western blotting analysis for FOXO3 and MyoG protein levels in both proliferating C2C12 cells (GM) and C2C12 cells that had undergone differentiation for 6 h in the presence of Nutlin-3 at 1-, 5- and 10-μM doses. (D) Western blotting analysis for FOXO3 ubiquitin levels in C2C12 cells that had been induced to differentiate for 3 h with the treatment of MG-132 (1 μM) or not. (E) Immunofluorescence staining of MHC (green) in myotubes that were treated by Nutlin-3 (at 1-, 5- and 10-μM doses) for the initial 24 h during differentiation process. The drug was then removed, and the differentiation continued until Day 7, at which point the samples were subjected to immunostaining. Nuclei were counterstained with DAPI (blue). Scale bar = 100 μm. The fusion index was quantified. (F) (left) Western blotting analysis for FOXO3 protein levels in DBC1 overexpression myotubes (differentiated for 7 days) with or without Nutlin-3 (10 μM) treatment for 24 h. (right) Immunofluorescence staining of MHC (green) in DBC1 overexpression myotubes (differentiated for 7 days) with or without Nutlin-3 (10 μM) treatment for 24 h. Nuclei were counterstained with DAPI (blue). Scale bar = 100 μm. Myotube length and diameter were quantified. *P* values were calculated using one-way ANOVA for multiple comparison (A, E).

proteins from differentiating C2C12 cells were heavily ubiquitinated (*Figure 7D*). Consistently, Nutlin-3 significantly inhibited the differentiation of C2C12 cells, as indicated by decreased fusion rates (*Figure 7E*). Similarly, high levels of DBC1 in myotubes could repress FOXO3 levels and improve myofibre quality, which can be reversed by Nutlin-3 treatment (*Figure 7F*). These data suggest that DBC1 controls ubiquitination-mediated FOXO3 degradation by positively regulating MDM2 expression from early stages of myogenesis until fully differentiated stage.

Discussion

In this study, we identified that DBC1 is essential for maintaining muscle mass by enhancing myogenesis and repressing myofibre wasting. Specifically, we found that DBC1 deletion in mouse skeletal muscle resulted in accelerated muscle loss, reduced muscle function and impaired muscle regeneration, all of which can be attributed to a common route of negatively regulating FOXO3. Further analysis showed that FOXO3 inhibited myogenesis by impairing mitochondrial functions

and accelerated myofibre wasting through activating the ubiquitin–proteasome and autophagy–lysosome pathways. This study provides both molecular and functional evidences that DBC1 may represent a key regulator of skeletal muscle atrophy that is caused by physiological or pathological factors.

Although previous research has linked DBC1 deletion to a significant reduction of muscle function,[16,17] this study is the first to elucidate the mechanism by which DBC1 maintains the integrity of skeletal muscle via promoting myogenesis of satellite cells and repressing myofibre wasting. Our findings indicate that DBC1 is consistently found reduced in degenerating skeletal muscles due to a variety of causes including ageing, immobilization or pharmacological side effects, suggesting a common underlying mechanism. DBC1 negatively regulated MDM2-mediated ubiquitination and degradation of FOXO3, which subsequently impaired mitochondrial functions during myogenesis and broke protein homeostasis in the mature myofibres. In adipose tissue, DBC1 has also been reported to have bifunctional roles in regulating adipocyte development and inflammation in fully differentiated 3T3-L1 adipocytes.[33,S17] These examples suggested that DBC1's function may vary depending on the development stages of cells. Most DBC1-related research to date has been conducted in cells that are either mitosis-competent or undifferentiated, so the role of DBC1 in terminally differentiated cells is poorly understood and requires further research in the future.

DBC1 is a known inhibitor of SIRT1, a key regulator of cellular functions such as metabolism, genomic stability and inflammation.[15] Prior research has shown that SIRT1 activation has negative effects on myogenesis. For example, SIRT1 activity declined when quiescent satellite cells activate to achieve metabolic reprogramming from oxidation to glycolysis upon activation.[30] SIRT1 activation mediated inhibition of myogenesis during glucose restriction[19] and repressed myotube formation through suppressing MyoD transcription.[34] Consistently, inhibition of SIRT1 activity by its inhibitor or hairpin RNA-mediated knockdown accelerated myogenesis.[19,30] In our study, we found that DBC1 knockdown impaired myogenesis, which is consistent with impaired myogenesis upon SIRT1 activation. However, inhibiting SIRT1 activity by Ex-527 or knocking down SIRT1 by hairpin RNA failed to rescue the impaired myogenesis (*Figure S7*), implying SIRT1 independence. Additionally, we found that DBC1 knockdown reduced mitochondrial functions, contrasting the previous finding that SIRT1 positively regulates mitochondrial biogenesis.[35] These evidences ruled out the possibility that loss of DBC1-impaired myogenesis was mediated by SIRT1 activation. Similarly, while SIRT1 has been shown to inhibit type I fibre atrophy during intermittent fasting[36] and prevented myotube wasting in the presence of high glucose by maintaining expression of slower fibre type MHC,[37] we found that DBC1 knockdown promoted myofibre wasting (*Figure 3*). Together, these findings suggest that the effects of DBC1 on myogenesis and myofibre maintenance are independent of SIRT1.

FOXO3 has been identified as an important regulator in maintaining quiescence of satellite cells,[22] although the underlying mechanisms are not yet fully understood. Mounting evidences suggest that mitochondria are important in controlling the fates of stem cells, including activation, self-renewal and differentiation.[38,S18] Mitochondrial dysfunctions have been shown to impair the myogenic capacity of satellite cells,[15,16] and inadequate mitochondrial activities resulting from ageing or genetic mutations can lead to failed myogenesis.[39,S19] This study reported that mitochondrial functions were suppressed in DBC1 knockdown myoblasts, and this was ascribed to elevated FOXO3, which led to reduced oxidative phosphorylation capacity and impaired myogenesis. Reducing FOXO3 protein levels in DBC1 knockdown cells restored mitochondrial functions and myogenesis (*Figures 4C,D* and *5*), demonstrating that FOXO3 regulates mitochondrial functions in DBC1-regulated myogenesis. The precise mechanism by which FOXO3 regulates mitochondrial functions is an intriguing subject that will be investigated more in the future.

In fully differentiated myofibres, mitochondrial dysfunctions are frequently observed during myofibre wasting.[40,S20] However, it is questionable whether there is a causality between mitochondrial dysfunctions and myofibre wasting, and if so, which one would be the cause. We also found that the metabolism was decreased in DBC1 knockdown myotubes (*Figure 3D–F*), which is indicative of mitochondrial dysfunctions. Furthermore, our data revealed that the FOXO3 protein levels were elevated in DBC1 knockdown myotubes, and we observed upregulated Atrogin1 and Murf1 expression, as well as increased conversion of LC3-I to LC3-II (*Figure 6A–C*). These findings are consistent with previous reports showing that FOXO3 upregulates atrophy-related genes such as Atrogin1 and Mur1, as well as activates autophagy.[S21] The degree of myofibre wasting was reduced in DBC1 knockdown cells by either blocking FOXO3's transcriptional activity or decreasing proteasome activity and autophagy flux, showing that FOXO3 mediates DBC1 ablation-induced myofibre wasting via activating ubiquitin–proteasome pathway and autophagy–lysosome pathway.

Skeletal muscle atrophy is a significant health concern that poses a challenge for clinical treatment. This study assessed the role of DBC1 in skeletal muscle atrophy by regulating satellite cell myogenesis and myofibre wasting. These findings revealed a previously unknown function of DBC1 in counteracting skeletal muscle atrophy and provided new insight for potential therapeutic approaches to treat muscle atrophy.

Acknowledgements

We thank Dr. Xiaoyue Wang's lab (Institute of Basic Medical Sciences, Chinese Academy of Medical Sciences and Peking Union Medical College) for assistance with analysis of RNA-sequencing data. The schematic is created with BioRender.com.

Conflict of interest statement

The authors report no conflicts of interest related to this work.

Data availability statement

All data are available in the main text or the supporting information.

Funding

This work was sponsored by CAMS Innovation Fund for Medical Sciences (2021-I2M-1-050 and 2022-I2M-1-012), National Key R&D Program of China (2022YFA1103803), the Non-profit Central Research Institute Fund of Chinese Academy of Medical Sciences (2022-JKCS-14) and the State Key Laboratory Special Fund (2060204).

Online supplementary material

Additional supporting information may be found online in the Supporting Information section at the end of the article.

References

1. Vinciguerra M, Musaro A, Rosenthal N. Regulation of muscle atrophy in aging and disease. *Adv Exp Med Biol* 2010;**694**: 211–233.
2. Larsson L, Degens H, Li M, Salviati L, Lee YI, Thompson W, et al. Sarcopenia: aging-related loss of muscle mass and function. *Physiol Rev* 2019;**99**:427–511.
3. Wall BT, Dirks ML, van Loon LJ. Skeletal muscle atrophy during short-term disuse: implications for age-related sarcopenia. *Ageing Res Rev* 2013;**12**:898–906.
4. Powers SK, Lynch GS, Murphy KT, Reid MB, Zijdewind I. Disease-induced skeletal muscle atrophy and fatigue. *Med Sci Sports Exerc* 2016;**48**:2307–2319.
5. Hernández-Hernández JM, García-González EG, Brun CE, Rudnicki MA. The myogenic regulatory factors, determinants of muscle development, cell identity and regeneration. *Semin Cell Dev Biol* 2017;**72**:10–18.
6. Chal J, Pourquié O. Making muscle: skeletal myogenesis in vivo and in vitro. *Development* 2017;**144**:2104–2122.
7. Chargé SB, Rudnicki MA. Cellular and molecular regulation of muscle regeneration. *Physiol Rev* 2004;**84**:209–238.
8. Hunt LC, Schadeberg B, Stover J, Haugen B, Pagala V, Wang YD, et al. Antagonistic control of myofiber size and muscle protein quality control by the ubiquitin ligase UBR4 during aging. *Nat Commun* 2021;**12**: 1418.
9. Fukada SI. The roles of muscle stem cells in muscle injury, atrophy and hypertrophy. *J Biochem* 2018;**163**:353–358.
10. Zhang H, Ryu D, Wu Y, Gariani K, Wang X, Luan P, et al. NAD^+ repletion improves mitochondrial and stem cell function and enhances life span in mice. *Science* 2016;**352**: 1436–1443.
11. Bodine SC, Latres E, Baumhueter S, Lai VK, Nunez L, Clarke BA, et al. Identification of ubiquitin ligases required for skeletal muscle atrophy. *Science* 2001;**294**: 1704–1708.
12. Cohen S, Nathan JA, Goldberg AL. Muscle wasting in disease: molecular mechanisms and promising therapies. *Nat Rev Drug Discov* 2015;**14**:58–74.
13. Sinha S, Elbaz-Alon Y, Avinoam O. Ca^{2+} as a coordinator of skeletal muscle differentiation, fusion and contraction. *FEBS J* 2022; **289**:6531–6542.
14. Nguyen NU, Wang HV. Dual roles of palladin protein in in vitro myogenesis: inhibition of early induction but promotion of myotube maturation. *PLoS ONE* 2015; **10**:e0124762.
15. Magni M, Buscemi G, Zannini L. Cell cycle and apoptosis regulator 2 at the interface between DNA damage response and cell physiology. *Mutat Res Rev Mutat Res* 2018;**776**:1–9.
16. Colman L, Caggiani M, Leyva A, Bresque M, Liechocki S, Maya-Monteiro CM, et al. The protein deleted in breast cancer-1 (DBC1) regulates vascular response and formation of aortic dissection during angiotensin II infusion. *Sci Rep* 2020;**10**:6772.
17. Kong S, Thiruppathi M, Qiu Q, Lin Z, Dong H, Chini EN, et al. DBC1 is a suppressor of B cell activation by negatively regulating alternative NF-κB transcriptional activity. *J Immunol* 2014;**193**:5515–5524.
18. Kim JE, Chen J, Lou Z. DBC1 is a negative regulator of SIRT1. *Nature* 2008;**451**: 583–586.
19. Fulco M, Cen Y, Zhao P, Hoffman EP, McBurney MW, Sauve AA, et al. Glucose restriction inhibits skeletal myoblast differentiation by activating SIRT1 through AMPK-mediated regulation of Nampt. *Dev Cell* 2008;**14**:661–673.
20. Braun T, Gautel M. Transcriptional mechanisms regulating skeletal muscle differentiation, growth and homeostasis. *Nat Rev Mol Cell Biol* 2011;**12**:349–361.
21. Mammucari C, Milan G, Romanello V, Masiero E, Rudolf R, Del Piccolo P, et al. FoxO3 controls autophagy in skeletal muscle in vivo. *Cell Metab* 2007;**6**:458–471.
22. Gopinath SD, Webb AE, Brunet A, Rando TA. FOXO3 promotes quiescence in adult muscle stem cells during the process of self-renewal. *Stem Cell Reports* 2014;**2**: 414–426.
23. Che J, Xu C, Wu Y, Jia P, Han Q, Ma Y, et al. Early-senescent bone marrow mesenchymal stem cells promote C2C12 cell myogenic differentiation by preventing the nuclear translocation of FOXO3. *Life Sci* 2021; **277**:119520.
24. Wiedmer P, Jung T, Castro JP, Pomatto LCD, Sun PY, Davies KJA, et al. Sarcopenia—molecular mechanisms and open questions. *Ageing Res Rev* 2021;**65**:101200.
25. Mehl KA, Davis JM, Berger FG, Carson JA. Myofiber degeneration/regeneration is induced in the cachectic $Apc^{Min/+}$ mouse. *J Appl Physiol (1985)* 2005;**99**:2379–2387.
26. Ma K, Mallidis C, Bhasin S, Mahabadi V, Artaza J, Gonzalez-Cadavid N, et al. Glucocorticoid-induced skeletal muscle atrophy is associated with upregulation of myostatin gene expression. *Am J Physiol Endocrinol Metab* 2003;**285**:E363–E371.
27. Biensø RS, Olesen J, Gliemann L, Schmidt JF, Matzen MS, Wojtaszewski JF, et al. Effects of exercise training on regulation of skeletal muscle glucose metabolism in elderly men. *J Gerontol A Biol Sci Med Sci* 2015;**70**:866–872.

28. Zhao W, Kruse JP, Tang Y, Jung SY, Qin J, Gu W. Negative regulation of the deacetylase SIRT1 by DBC1. *Nature* 2008;**451**:587–590.
29. Ferber EC, Peck B, Delpuech O, Bell GP, East P, Schulze A. FOXO3a regulates reactive oxygen metabolism by inhibiting mitochondrial gene expression. *Cell Death Differ* 2012;**19**:968–979.
30. Ryall JG, Dell'Orso S, Derfoul A, Juan A, Zare H, Feng X, et al. The NAD^+-dependent SIRT1 deacetylase translates a metabolic switch into regulatory epigenetics in skeletal muscle stem cells. *Cell Stem Cell* 2015;**16**:171–183.
31. Salcher S, Spoden G, Hagenbuchner J, Führer S, Kaserer T, Tollinger M, et al. A drug library screen identifies carbenoxolone as novel FOXO inhibitor that overcomes FOXO3-mediated chemoprotection in high-stage neuroblastoma. *Oncogene* 2020;**39**:1080–1097.
32. Yang JY, Zong CS, Xia W, Yamaguchi H, Ding Q, Xie X, et al. ERK promotes tumorigenesis by inhibiting FOXO3a via MDM2-mediated degradation. *Nat Cell Biol* 2008;**10**:138–148.
33. Moreno-Navarrete JM, Moreno M, Vidal M, Ortega F, Ricart W, Fernández-Real JM. DBC1 is involved in adipocyte inflammation and is a possible marker of human adipose tissue senescence. *Obesity (Silver Spring)* 2015;**23**:519–522.
34. Fulco M, Schiltz RL, Iezzi S, King MT, Zhao P, Kashiwaya Y, et al. Sir2 regulates skeletal muscle differentiation as a potential sensor of the redox state. *Mol Cell* 2003;**12**:51–62.
35. Tang BL. Sirt1 and the mitochondria. *Mol Cells* 2016;**39**:87–95.
36. Lee D, Goldberg AL. SIRT1 protein, by blocking the activities of transcription factors FoxO1 and FoxO3, inhibits muscle atrophy and promotes muscle growth. *J Biol Chem* 2013;**288**:30515–30526.
37. Dugdale HF, Hughes DC, Allan R, Deane CS, Coxon CR, Morton JP, et al. The role of resveratrol on skeletal muscle cell differentiation and myotube hypertrophy during glucose restriction. *Mol Cell Biochem* 2018;**444**:109–123.
38. Hori S, Hiramuki Y, Nishimura D, Sato F, Sehara-Fujisawa A. PDH-mediated metabolic flow is critical for skeletal muscle stem cell differentiation and myotube formation during regeneration in mice. *FASEB J* 2019;**33**:8094–8109.
39. Hong X, Isern J, Campanario S, Perdiguero E, Ramírez-Pardo I, Segalés J, et al. Mitochondrial dynamics maintain muscle stem cell regenerative competence throughout adult life by regulating metabolism and mitophagy. *Cell Stem Cell* 2022;**29**:1298–314.e10.
40. Bua EA, McKiernan SH, Wanagat J, McKenzie D, Aiken JM. Mitochondrial abnormalities are more frequent in muscles undergoing sarcopenia. *J Appl Physiol (1985)* 2002;**92**:2617–2624.